



# Quantitative transcriptomics, and lipidomics in evaluating ovarian developmental effects in Atlantic cod (*Gadus morhua*) caged at a capped marine waste disposal site

Essa A. Khan<sup>a</sup>, Xiaokang Zhang<sup>b</sup>, Eileen M. Hanna<sup>b</sup>, Zdenka Bartosova<sup>c</sup>, Fekadu Yadetie<sup>d</sup>, Inge Jonassen<sup>b</sup>, Anders Goksøyr<sup>d</sup>, Augustine Arukwe<sup>a,\*</sup>

<sup>a</sup> Department of Biology, Norwegian University of Science and Technology (NTNU), N-7491, Trondheim, Norway

<sup>b</sup> Computational Biology Unit, Department of Informatics, University of Bergen, N-5008, Bergen, Norway

<sup>c</sup> Department of Biotechnology and Food Science, NTNU, N-7491, Trondheim, Norway

<sup>d</sup> Department of Biological Sciences, University of Bergen, N-5020, Bergen, Norway

## ARTICLE INFO

### Keywords:

RNA-Seq  
Lipid profile  
Ovarian development  
Reproduction  
Teleost  
Environmental pollution

## ABSTRACT

In the present study, a previously capped waste disposal site at Kollevåg (Norway) was selected to study the effects of contaminant leakage on biomarkers associated with Atlantic cod (*Gadus morhua*) reproductive endocrinology and development. Immature cod were caged for 6 weeks at 3 locations, selected to achieve a spatial gradient of contamination, and compared to a reference station. Quantitative transcriptomic, and lipidomic analysis was used to evaluate the effects of the potential complex contaminant mixture on ovarian developmental and endocrine physiology. The number of expressed transcripts, with 0.75 log<sub>2</sub>-fold differential expression or more, varied among stations and paralleled the severity of contamination. Particularly, significant bio-accumulation of  $\sum$ PCB-7,  $\sum$ DDTs and  $\sum$ PBDEs were observed at station 1, compared to the other station, including the reference station. Respectively 1416, 698 and 719 differentially expressed genes (DEGs), were observed at stations 1, 2 and 3, compared to the reference station, with transcripts belonging to steroid hormone synthesis pathway being significantly upregulation. Transcription factors such as *esr2* and *ahr2* were increased at all three stations, with highest fold-change at Station 1. MetaCore pathway maps identified affected pathways that are involved in ovarian physiology, where some unique pathways were significantly affected at each station. For the lipidomics, sphingolipid metabolism was particularly affected at station 1, and these effects paralleled the high contaminant burden at this station. Overall, our findings showed a novel and direct association between contaminant burden and ovarian toxicological and endocrine physiological responses in cod caged at the capped Kollevåg waste disposal site.

## 1. Introduction

In teleosts, reproductive development is a dynamic process throughout ontogeny by either progressing or regressing and controlled by a complex set of pathways that require communication and interaction along system axes (Martyniuk et al., 2013). As a result, several hormones and other physiological systems that are not normally associated with reproductive development play significant roles in ensuring that offspring are produced at a time of the year optimal for their survival (Davis et al., 1994). Therefore, reproduction is susceptible to contaminant exposure at several developmental stages including

energetic adaptation, sexual maturation, zonagenesis and vitellogenesis, oocyte maturation, fertility and fertilization (Arukwe and Goksøyr, 2003). The internal responses that are synchronized by external signals during sexual maturation are dependent on a genetically determined performance threshold. Thus, maturation processes can only proceed, if this performance exceeds a set point at a critical time in winter or spring (Thorpe, 1994). The maturation processes and the associated energetic demand can be altered by contaminant exposure with potentially deleterious ecological consequences (Hamilton et al., 2017).

Historically and based on “out of sight and out of mind” principle, household and industrial wastes were deposited into oceans (Goldberg,

\* Corresponding author.

E-mail address: [augustine.arukwe@ntnu.no](mailto:augustine.arukwe@ntnu.no) (A. Arukwe).

<https://doi.org/10.1016/j.envres.2020.109906>

Received 5 May 2020; Received in revised form 29 May 2020; Accepted 1 July 2020

Available online 12 July 2020

0013-9351/© 2020 The Author(s). Published by Elsevier Inc. This is an open access article under the CC BY license (<http://creativecommons.org/licenses/by/4.0/>).

1981). A major concern with this dumping practice is that these wastes contain complex mixtures of environmental pollutants, including organochlorine pesticides (OCPs), polycyclic aromatic hydrocarbons (PAHs), polychlorinated biphenyls (PCBs), heavy metals, pharmaceuticals and personal care products (PPCPs), per- and polyfluoroalkyl substances (PFASs), organophosphate esters (OPEs), among others (Chrysikou et al., 2008; Vassenden and Johannessen, 2009). Aquatic organisms, especially fish, bioaccumulate these pollutants and are therefore, an important biota for ecological risk assessment. The reason for this is that, these contaminants may interfere or alter hormonal systems, which in turn modulate different physiological processes, such as gonadal differentiation and development, and ultimately reproductive output (Orn et al., 2006).

The Kollevåg bay is located off the city of Bergen, Norway. From 1930 to 1975, this site was used for disposing industrial and household wastes. After terminating the dumping practice, the site was capped by sand and stone, and later by tarpaulin after a routine monitoring reported the leaching of contaminants and their presence in fish caught at the area in 2004 (Vassenden and Johannessen, 2009). Given that the Kollevåg bay was developed into a popular beach and recreational site, leaching of contaminants from this area represents significant environmental, biota and human health issues of serious concerns. Therefore, sites (presented in SI Fig. S1) along the gradient of contamination at Kollevåg were selected for *in situ* caging. The present study is based on our previous report showing the bioaccumulation of different contaminants in cod tissue after caging at the Kollevåg stations (Dale et al., 2019). For example, biliary hydroxylated (OH) PAH metabolites were significantly higher at all Kollevåg stations, compared to the reference station. On the other hand, the liver only showed significantly higher levels of  $\Sigma$ PCB-7, dichlorodiphenyltrichloroethane ( $\Sigma$ DDTs) and polybrominated diphenyl ethers ( $\Sigma$ PBDEs) at station 1, compared to the reference station (Dale et al., 2019). We also reported strong relationships between the alteration of ovarian steroidogenesis and other reproductive biomarkers with the bioaccumulation of environmental contaminants in fish tissues from the Kollevåg stations (Dale et al., 2019). These findings highlighted the need for further investigation of overt biological processes that may be altered during fish ovarian development.

Therefore, our aim with the present study was to apply the sensitivity of transcriptome sequencing and non-target lipidomic approach in evaluating changes in broad-scale transcripts and metabolic profile in female cod caged at the capped Kollevåg waste disposal site. We tested the hypothesis that molecular and metabolic responses or mechanisms of action in fish ovaries represent significant and valuable endpoints in evaluating the effects of bioactive chemicals in complex mixtures. These responses and mechanisms will ultimately be ignored by evaluating individual transcripts and protein responses under such exposure conditions.

## 2. Materials and methods

### 2.1. Chemicals and reagents

Direct-zol RNA isolation and MiniPrep kit from Zymo Research Corporation (Irvine, CA, U.S.A.), iTaq SYBR Green Supermix with ROX and iScript cDNA synthesis Kit were purchased from Bio-Rad Laboratories (Hercules, CA, U.S.A.).

### 2.2. Site selection and fish exposure

Detailed information about the study site selection, fish and exposure conditions are reported in Dale et al. (Dale et al., 2019) (SI Fig. S1A). In brief, juvenile Atlantic cod approximately 1.5 years old were used for this experiment. Each cage consisted of 22 individuals and were placed at three different locations in or near the waste disposal site at Kollevåg, Askøy. Station 1 is located at the capped area in Vestrevågen (V). Station

2 is at the borderline between Vestrevågen and Medavågen (M) and station 3 is at the outer parts of Kollevåg (see SI Fig. S1A). One cage was placed at the reference station, located close to Ertenøyane (SI Fig. S1A). Ambient temperature was determined both during deployment and retrieval of the cages, at the range of 11 °C–15 °C. The cod were caged for six weeks from early September to mid-October 2016 followed by euthenization and tissues collection for downstream analysis. The sex of the fish was determined by inspection of the gonads after dissection, and only female ovaries were used for this study. Post-caging changes in the ovarian condition of female cod were determined by gonadosomatic index (GSI), showing no significant differences between the reference and Kollevåg stations, as presented in Supporting Information (SI Figure S2.1).

### 2.3. RNA extraction and sequencing

RNA was extracted from frozen ovarian tissues (n = 3–5 per site) using Direct-zol<sup>TM</sup> RNA extraction kit, followed by RNA quantification using NanoDrop ND-1000 spectrophotometer (NanoDrop Technologies, Wilmington, DE, USA). RNA integrity assessment was attempted using an Agilent 2100 Bioanalyzer (Agilent Technologies, Palo Alto, CA), however, RNA integrity numbers could not be calculated due to unusual RNA composition (Kroupova et al., 2011), presented in SI Figure S2.2. Complementary DNA (cDNA) library was prepared by following the guideline of TruSeq<sup>®</sup> Stranded mRNA Preparation Kit. Poly(A)<sup>+</sup> RNA purified from total RNA (400 ng) was fragmented and converted to cDNA strand that, after a 15 cycle PCR amplification, resulted to the final cDNA library for sequencing. Illumina HiSeq 4000 (Illumina, Inc., San Diego, CA, USA) platform was used to sequence cDNA library to generate 75 bp paired-end reads of 50 million depth.

### 2.4. Differential expression analysis (DEA)

The pipeline used for differential expression analysis (DEA) is available at <https://github.com/zhexiaokang/RASflow>, starting with a quality control using FastQC v0.11.5 tool (<http://www.bioinformatics.babraham.ac.uk/project/fastqc>) and aligning clean reads against 22,154 published Atlantic cod CDS available at [ensembl.org \(ftp://ftp.ensembl.org/pub/release-90/fasta/gadus\\_morhua/cds/Gadus\\_morhua.gad\)](http://ftp.ensembl.org/pub/release-90/fasta/gadus_morhua/cds/Gadus_morhua.gad) using HISAT2 v2.1.0 tool (Zhang and Jonassen, 2020). Read counts were generated using SAM tools v1.4.1. Genes that passed the threshold count per million (cpm) of  $\geq 1$ , at least two samples per comparison (between Kollevåg and reference stations) were selected for differential analysis. About, 13366, 13393 and 13202 transcripts were shortlisted while respectively comparing Kollevåg station 1, 2 and 3 with the reference station. To check the correlation between the biological replicates at each station in cpm values were used to construct scatter plots and Pearson correlation was performed (SI Fig. S3). Correlation coefficient (R) for each group was observed in the range of 0.86–0.99, 0.98–0.99, 0.90–0.98 and 0.97–0.98 at the reference site, Stations 1, 2 and 3, respectively. Differential expression of transcripts between Kollevåg and reference stations were determined using DESeq v1.24.0 tools. Furthermore, we performed “TMM” normalization and adjusted statistical p-value (p-adj) using the Benjamini-Hochberg multiple testing correction. A threshold of log<sub>2</sub> fold-change of 0.75 (1.68-fold change) for upregulated and –0.75 (0.59-fold change) for downregulated transcripts and p-adj < 0.05 were set. The RNA-seq data have been deposited in European Nucleotide Archive (ENA) with accession number - PRJEB34872.

### 2.5. Pathway analysis

For pathway enrichment analysis, MetaCore<sup>TM</sup> version 6.30 (<http://portal.genego.com/>), a Thomson Reuter's business pathway maps were used to identify different pathways or processes that are significantly affected at Kollevåg stations. The level of significance was determined

by inbuilt software functions, using Fishers's exact test variations adjusted for multiple sample testing by Benjamini-Hochberg false discovery ratio (FDR) analysis. A threshold FDR for significantly affected pathways were set at <0.05. In MetaCore, human (*Homo sapiens*) orthologs of Atlantic cod transcripts were extracted and used, using the BioMart tool in Ensembl (<http://www.ensembl.org>).

## 2.6. Lipidomics

Non-targeted lipid analysis of ovarian tissue was performed using an Ultrahigh-performance supercritical fluid chromatography (UPC2®) coupled to a hybrid quadrupole orthogonal time-of-flight mass spectrometer SYNAPT G2-S HDMS (both Waters, Milford, MA, USA). A previously described separation method of Lisa and Holčapek (Lisa and Holčapek, 2015) was used with some modifications. Chromatographic conditions and detection settings are listed in SI Section 4.1. A Precellys® 24 bead homogenizer with a Cryolys cooling system (all Bertin Technologies SAS), have been employed for tissue homogenization and a solvent system previously described by Folch et al. (Folch et al., 1957) has been used for lipid extraction. Snap frozen ovarian tissue (50 mg) was homogenized with zirconium oxide beads ( $0.5 \pm 0.01$  g,  $\emptyset$  1.4 mm) in 400  $\mu$ L of a cold mixture of chloroform/methanol (2:1, v/v). Two bead-beating cycles (6500 rpm, 20s) were applied to obtain a homogeneous sample. An addition of 600  $\mu$ L of a cold mixture of chloroform/methanol (2:1, v/v) followed and tubes were shaken for 10 min using a thermo-shaker (Thermal shake lite, VWR). Phase separation was induced by adding 200  $\mu$ L of water. Shaking cycle was repeated and centrifuge were subsequently used for phase separation. A chloroform layer containing lipids was collected and filtered through a syringe filter with PTFE membrane, 0.2  $\mu$ m,  $\emptyset$  13 mm (VWR International). Final extracts were stored at  $-20$  °C in glass vials until analyzed with UPC<sup>2</sup>-MS/MS. Dichloromethane was used as a sample diluent prior to injection. Detailed experimental conditions and data processing are presented in SI Section 4.1.

## 2.7. Quantitative (real-time) PCR

For qPCR, cDNA was synthesized from 1  $\mu$ g total RNA, following the instruction of the iScript cDNA synthesis kit (Bio-Rad, Hercules, CA, USA). PCR reaction mix (20  $\mu$ L) containing 5  $\mu$ L of 1:6 diluted cDNA, 0.5  $\mu$ M each of the forward and reverse primers were amplified using Mx3000P real-time PCR machine (Stratagene, La Jolla, CA). A detailed protocol for qPCR measurements of gene expression is presented in SI Section 4.2. Primer pair sequences used for transcript amplification are shown in SI Table S3.

## 2.8. Statistical analysis

Statistical analysis of log<sub>2</sub>-transformed fold-changes of gene expression from qPCR was performed on IBM SPSS Statistics 25. The statistical difference between reference and Kollevåg stations were determined using one-way ANOVA (post-hoc Dunnett's test) with the significance level set at  $\alpha = 0.05$ . The vast majority of transcripts were normally distributed, except *aldh16a1*, *hsp12b*, and *mgst3a*. To normalize the residuals of the model, *aldh16a1* and *hsp12b* were transformed using natural logarithm and *mgst3a* by square root transformation. This was statistically inspected using Shapiro-Wilk and Kolmogorov-Smirnov test. Only *foxo1* and *plpp1* violated Shapiro-Wilk test, and we therefore applied Kolmogorov-Smirnov test to check normality. The homogeneity of variance was determined by Levene's test. The *cyp11c1*, *hsp12b*, *mgst3a*, *plpp1*, *pik3r2* and *stat6* data violated Levene's homogeneity, therefore Welch's heteroscedastic F-test and Brown-Forsythe test was applied. Graphs are plotted using GraphPad Prism 5 (version 5.01) and ShinyCircos: an R/Shiny application for interactive creation of Circos plot.

## 3. Results

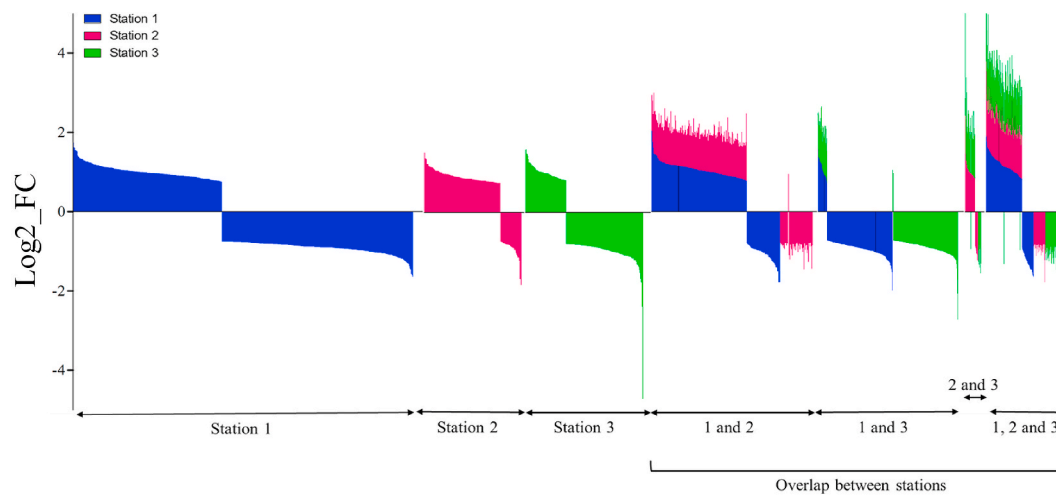
### 3.1. Transcript changes in cod ovary

Compared to the reference station, Kollevåg station 1, 2 and 3 showed respective 1416, 698 and 719 DEGs, with  $p < 0.05$ , based on RNA sequencing. Out of the 1416 cod DEGs at Station 1, 47.6% and 52.4% were up- and down-regulated, respectively. A large number (77%) of DEGs at Station 2 were up-regulated, and the remaining 23% are down-regulated. In contrast, Station 3 contained a reduced number of up-regulated (37.6%) and a larger number of down-regulated (62.4%) DEGs (Fig. 1). Some of the DEGs were common among stations. The innermost station (i.e. Station 1) shared 435 DEGs with Station 2 and 450 with Station 3. Of these, 161 transcripts were common among all three Kollevåg stations (Fig. 1). A group of DEGs with shared unique counterparts among stations, that either violated threshold log<sub>2</sub> fold-change or p-adj values are shown in SI Table S1. Not all cod DEGs orthologs were identified in Humans (*Homo sapiens*) genome available at Ensembl (<http://www.ensembl.org>). Only 1008 human orthologs of the 1416 cod DEGs were identified at Station 1, while Station 2 and 3 contained 525 and 584 identified transcripts, respectively. Some transcripts in cod have more than one ortholog in humans and vice versa. For example, *si:ch73-206p6.1* cod gene has four orthologs in humans, including phospholipid scramblase 2 (*plscr2*), *plscr3*, *plscr4* and *plscr5* (SI Table S1).

### 3.2. Functional enrichment of DEGs in cod ovary

To understand the biological implication of cod DEGs, functional enrichment analysis was performed to identify pathways significantly affected at Kollevåg stations. Overall, the number of enriched pathways decreased from Stations 1 to station 3, as shown in SI Table S2. In this study, pathways were shortlisted based on their relevance with different biological processes that are important for ovarian physiology and development. This includes pathways associated with translation, transcription, signal transduction, oxidative stress, ovarian cancer, lipid metabolism, G-protein signaling, apoptosis, epithelial to mesenchymal transition (EMT), DNA damage, cytoskeleton remodelling, cell adhesion and immune system (Fig. 2). A large number of these pathways were significantly affected at Station 1  $> 2 > 3$ , compared to the reference station. Their log<sub>10</sub>\_FDR falls at or across threshold level, set at  $-1.3$  (Fig. 2).

The outcome of significantly affected biological pathways were dependent on the expression pattern of DEGs, which is similar among Kollevåg stations, but with differential expression levels (SI Figure S4a-e, S7, S8, and S9). Despite few exceptions, majority of the transcripts at Station 1 showed higher fold-change in their differential expression pattern, than the other two stations. These observations followed the pattern of contaminant loading including - DDTs, PBDEs, and PCBs that were present at Station 1, compared to OH-PAH metabolites that was common at all Kollevåg stations. For example, lipid metabolism, cellular pathways for arachidonic acid (ARA) biosynthesis and its metabolite production were significantly affected at Station 1 and 2 (Fig. 3). Phospholipase A2 group IVA (*pla2g4a*), an important enzyme for ARA biosynthesis was upregulated at both Stations 1 and 2, but no significant change was observed at Station 3. However, mitogen activated protein kinase 1 (*mapk1*) was significantly present at all three stations, despite the fact that Station 3 does not show any response towards the biosynthesis of ARA. Other important transcripts including phospholipid phosphatase 1 (*plpp1*), *plpp3* and amyloid- $\beta$  precursor protein (*app*) showed similar expression pattern at both Station 1 and 2, with implication for the production of ARA by ACM receptor. Other sets of transcripts such as protein kinase C delta (*prkcd*), guanine nucleotide binding protein (G protein),  $\beta$ -polypeptide 2 (*grb2*) and inositol 1,4,5-trisphosphate receptor, type 2 (*itpr2*) were not associated with this pathway, due to their significant differential presence at Station 3 only



Differentially expressed genes (DEGs)	Number and %-age of DEGs at			DEGs overlap between stations			
	Station 1	Station 2	Station 3	1 and 2	1 and 3	2 and 3	1, 2 and 3
Up-regulated	674 (47.6%)	538 (77%)	270 (37.6%)	324	158	156	120
Down-regulated	742 (52.4%)	160 (23%)	449 (62.4%)	111	292	50	41
<b>Total</b>	<b>1416</b>	<b>698</b>	<b>719</b>	<b>435</b>	<b>450</b>	<b>206</b>	<b>161</b>

**Fig. 1.** Ovarian gene expression profile of female juvenile cod caged along a contaminant gradient at three Kollevåg stations, relative to the reference station. Quantitative expression analysis by RNA sequencing, showing only significant differentially expressed genes (DEGs) was organized based on their expression levels with log<sub>2</sub>FC threshold set at +0.75 and -0.75. Some cod DEGs that are common between stations were organized into four groups with varying overlap. Stack representation in overlap section is for up-regulated genes. However, down-regulated genes are plotted with their original Log<sub>2</sub>FC values without putting them in a stack. For clarity, actual numbers and %-age of cod DEGs at each station are presented in the table below.

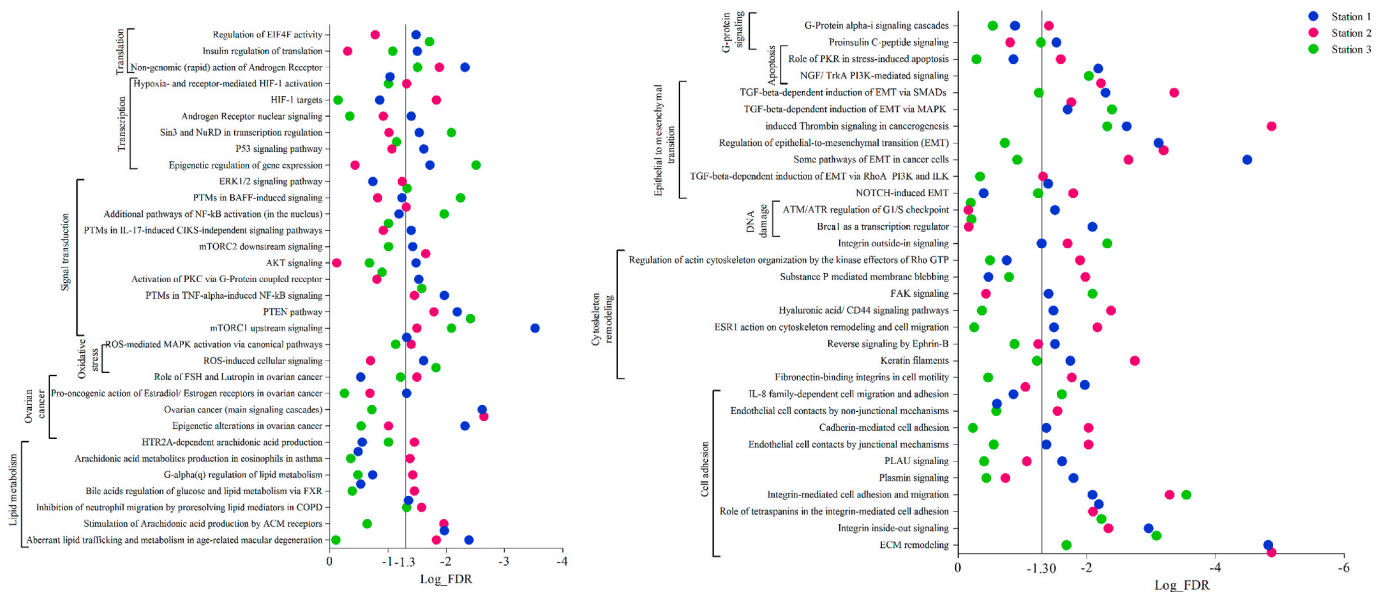


**Fig. 2.** Predicted biological processes and associated pathways affected in the ovary of female juvenile cod caged at Kollevåg stations using Metacore software. Adjusted p-value (FDR) of each pathway is plotted in scatter biplot; blue, red and green dots represent station 1, 2 and 3 respectively. The X-axis is a log<sub>10</sub>FDR and the threshold line drew at -1.3. (For interpretation of the references to color in this figure legend, the reader is referred to the Web version of this article.)

(Fig. 3). The majority of ARA metabolite producing pathway transcripts, were common between Station 1 and 2, except prostaglandin-endoperoxide synthase 1 (*ptgs1*) that was significantly present at Station 2 only. Guanine nucleotide binding protein (G protein) alpha 12a (*gna12*), together with G protein subunit alpha o1 (*gnao1*), *mapk1* and

*pla2g4a* were significantly affected by HTR2A dependent ARA production pathway (Fig. 3). Other lipid metabolic pathways were affected differently at the stations, depending on the presence of their associated transcripts at differential significant levels.



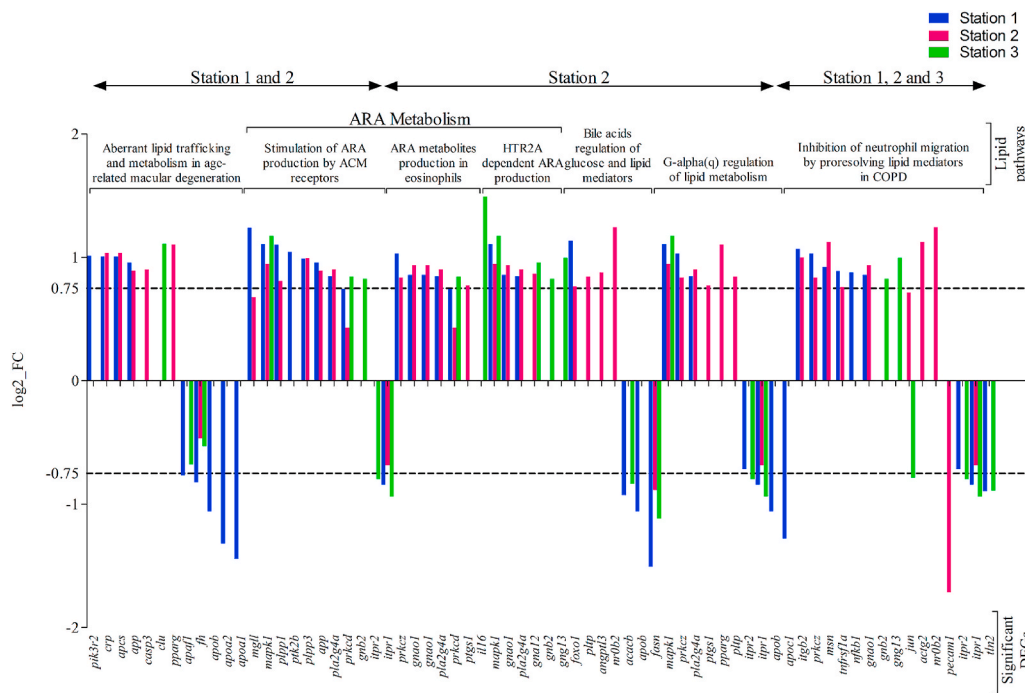


**Fig. 3.** Genes associated with different cellular pathways of lipid metabolism specifically affected in the ovary of juvenile female cod caged at different Kollevåg stations. DEGs that are statistically significant and there log<sub>2</sub>\_FC across threshold set at +0.75 and -0.75, is presented in color bars. (For interpretation of the references to color in this figure legend, the reader is referred to the Web version of this article.)

3.3. Lipidomics and relevance to transcriptomics in cod ovary

To investigate the association between transcriptional changes and levels of functional metabolites, we applied non-targeted UPC<sup>2</sup>-MS/MS

approach to reveal changes in the lipidome. Differential lipid levels were determined by comparing the mean abundance of particular lipid species at each Kollevåg station, relative to the reference station. Differential abundance of lipid species at Kollevåg stations is presented in a

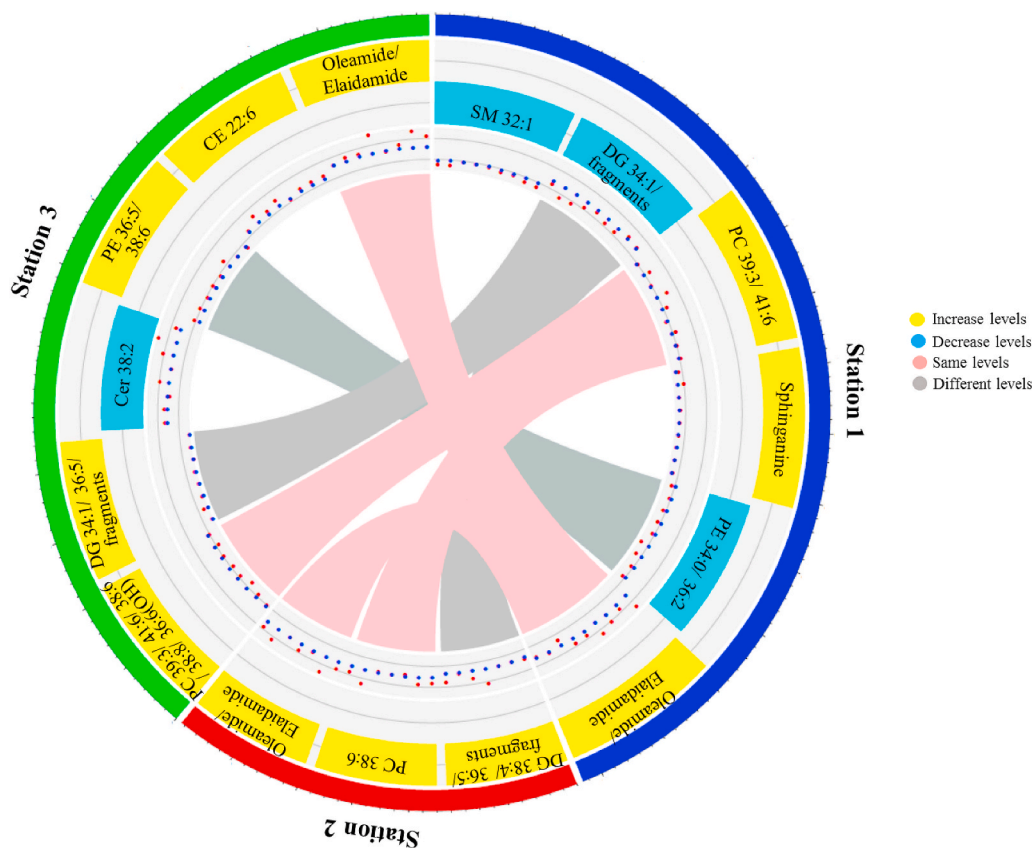


**Fig. 4.** Chord diagram indicating variations in abundance of lipid compounds in ovaries from female juvenile cod caged at Kollevåg stations. The abundance of particular lipid species in each sample at each Kollevåg station is presented in a scatter plot (red) compared to mean abundance of that species at reference station (blue). In comparing their abundance, lipid species with low and high levels at Kollevåg stations are presented in cyan and yellow bars respectively. Inter-station connection bands with different colors show either same or different levels of lipid between station1 and other two. (For interpretation of the references to color in this figure legend, the reader is referred to the Web version of this article.)

chord diagram as shown in Fig. 4 and SI Section 6.1a-c. Some lipid species belonging to sphingolipids were differentially present at Station 1 and 3 only. The innermost station (i.e. Station 1) showed decreased and increased levels of sphingomyelin (SM) 32:1 and C17 sphinganine, respectively. Whereas, ceramide (Cer) 38:2 levels decreased only at Station 3. Species of diacylglycerol (DG 34:1, DG 36:5, DG 38:4), glycerophosphocholine (PC 38:6, PC 38:8, PC 39:3, PC 41:6 and PC 36:6 (OH)) and fatty amides (Oleamide/Elaidamide) were differentially present at all three stations. Species of DG decreased at Station 1 and increased at stations 2 and 3, whereas lipid species belonging to PC and fatty amide class increased at all stations. Phosphoethanolamine (PE) and DG levels decreased and increased at station 1 and 3, respectively. Cholesterol ester (CE 22:6) is another unique lipid present only at Station 3 (Fig. 4). The unique relationship between observed differential abundance of lipid species and individual lipids at each station is presented in the principal component analysis (PCA) biplots shown in SI Figs. S5a-c.

### 3.4. RNA-seq validation

RNA-seq data were verified by RT-qPCR of eleven randomly selected transcripts. The results are presented in bar charts (Fig. 5), as well as correlation-plot between the log<sub>2</sub> fold-change values obtained from the RT-qPCR and RNA-seq data (Fig. 6). The Pearson correlation coefficient,  $r = 0.824$  ( $p < 0.0001$ ), showed strong positive relationships between these approaches as shown in Fig. 6.

## 4. Discussion

The bay of Kollevåg, previously used as a marine waste dumping site provided a unique opportunity for investigating changes in biological responses to complex mixture of contaminants. Earlier, Dale, et al. (Dale et al., 2019) reported transcriptional changes of hepatic

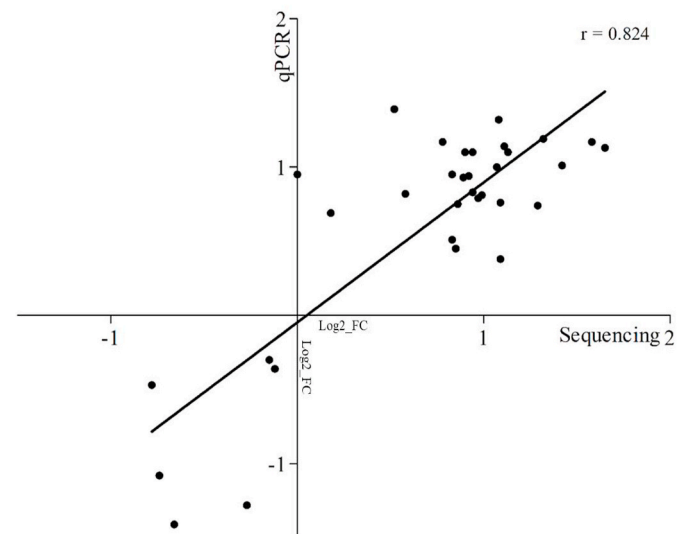


Fig. 6. RT-qPCR validation of differentially expressed RNA sequencing genes, in juvenile cod ovaries from Kollevåg stations. The linear regression line represents positive association at significant Pearson correlation coefficient,  $r = 0.824$  ( $p < 0.0001$ ).

biotransformation and ovarian steroidogenesis in relation to accumulated contaminants in cod tissues, after a six-week caging period. These findings prompted us to study other biological processes influenced by this exposure to ovarian tissue. Thus, we present and discuss how differentially expressed cod ovarian transcripts may possibly affect the output of cellular pathways that are important for reproductive physiology and toxicology in teleosts.

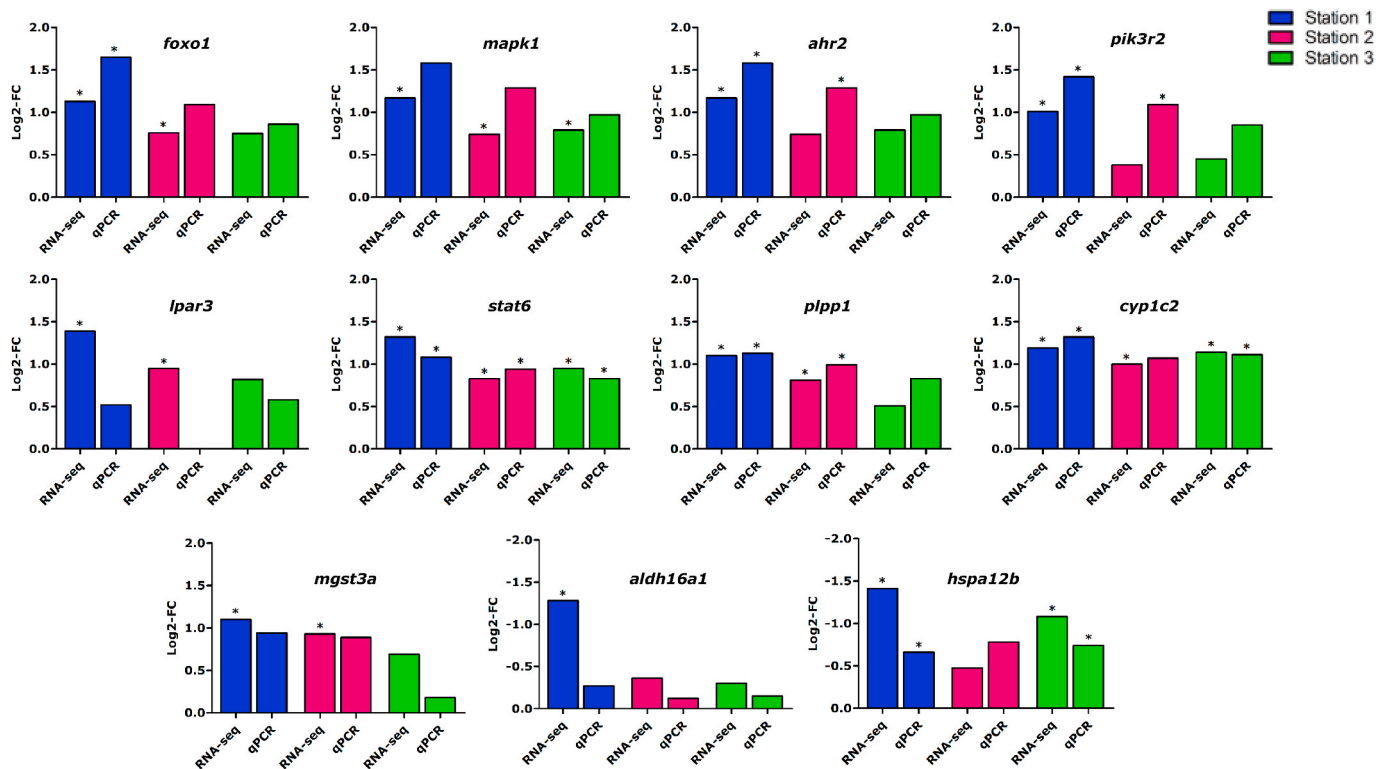


Fig. 5. Significant/non-significant log<sub>2</sub>-FC, from RNA-seq and RT-qPCR of *foxo1*, *mapk1*, *ahr2*, *pik3r2*, *lpar3*, *stat6*, *cyp1c1*, *plpp1*, *mgst3a*, *aldh16a1* and *hspa12b* genes at each station. Log<sub>2</sub>-FC in mRNA levels of these genes from RNA sequencing and qPCR, were plotted in parallel. RNA sample for qPCR were taken from 7 to 8 fish per station. Log<sub>2</sub>-FC were calculated based on mean expression of their mRNA at the stations. Significant change in expression are represented with asterisk (\*),  $p < 0.05$ .

#### 4.1. Biological processes and associated pathways

##### 4.1.1. Relationship between contaminant burden and DEGs at Kollevåg stations

As reported in Dale et al. (Dale et al., 2019), bile and liver contaminant burden at the three Kollevåg stations showed a decreasing concentration gradient from the innermost (Station 1) to the outermost (Station 3) stations. The detection of significantly, higher biliary concentration of OH-PAH metabolites (1-OH-phenanthrene, 1-OH-pyrene and 3-OH-benzo[a]pyrene) at Kollevåg stations, compared to the reference station, also demonstrated the bioavailability of these contaminants to the experimental cod. Further, the pattern of contaminants in the liver of cod at the Kollevåg stations paralleled the number of DEGs at the individual stations and their overlaps, as shown in Fig. 1. The highest number of cod DEGs were observed at station 1 and this observation also paralleled the liver burden for  $\sum$ PCB-7,  $\sum$ DDTs and  $\sum$ PBDEs that were recorded at the highest concentrations at station 1. Based on the above gradient relationship between contaminant at the Kollevåg, further discussion on biological processes and associated pathways will assume this premise in evaluating DEGs to complex contaminant mixture at the sites, relative to the reference station.

##### 4.1.2. Modulation of transcripts of Pkr and Ngf/TrkA PI3k apoptotic pathway

Higher expression of both tumor necrosis factor receptor 1 (Tnfr1) and caspase-3 (Casp3) promotes ovarian granulosa cell death (Boone and Tsang, 1998). The caspase cascade promotes its activity by targeting the expression of Tnfr-associated factor 6 (Traf6) (Chen et al., 2015). The Pkr stress-induced apoptotic pathway was affected only at Station 2, due to significantly higher expression levels of *cas3* mRNA, than other two stations. The expression of *cas3* followed the abundance of OH-PAH metabolites accumulated in cod tissue at Kollevåg stations. This observation was further supported by the findings of Lim et al. (Lim et al., 2016), showing that BaP exposure increased caspase-dependent germ cell apoptosis in mouse fetal ovary. Furthermore, the expression of both *tnfr1* and *traf6* followed the same pattern, that was previously reported by Boone and Tsang (1998) and Chen et al. (Chen et al., 2015), that augments ovarian apoptosis (SI Fig. S4a). Other transcripts of apoptotic pathways, including eukaryotic translation initiation factor 2 alpha kinase 2 (*eif2ak2*) and *mapk1* were highly expressed at Kollevåg stations (SI Fig. S4a). In general, these transcripts have been shown to boost apoptosis by enhancing the transcriptional activity of the tumor suppressor p53 (Cuddihy et al., 1999; Yeh et al., 2001). Further, Ngf/TrkA PI3k-mediated apoptotic pathway was significantly affected at all three stations (SI Fig. S4a). Most of the transcripts associated with this pathway were significantly affected and their differential levels of expression at Kollevåg stations paralleled types and abundance of contaminants in cod tissues.

A significant decrease in the expression of *notch2* mRNA was observed at Kollevåg stations that correlated with increased levels of PAH metabolites detected in cod bile as demonstrated in the PCA shown in SI Tables S1–B. The *notch2* knockout mice showed ovarian carcinogenesis that included a reduction in the number of both primordial and antral follicles and decreased proliferation of granulosa cells (Vanorny et al., 2014). Previously, exposure of rat to the PAH, 3-methylcholanthrene (3-MC) produced follicular composition of *notch2* knockout animal (Rhon-Calderón et al., 2018).

##### 4.1.3. Transcriptional alteration of Brca1, Atm/Atr pathway associated transcripts for DNA damage

Accumulation of persistent organic pollutants (POPs) induce DNA lesions and dysregulate pathways responsible for repairing DNA damage (He et al., 2015). In the present study, DNA damage pathways such as “Brca1 as a transcription regulator” and “Atm/Atr regulation of G1/S checkpoints” were significantly affected, only at Kollevåg station 1 (SI Fig. S4b). Previously, Fabbro, et al. (Fabbro et al., 2004) reported the

importance of both breast and ovarian cancer susceptibility protein 1 (Brca1) and ataxia-telangiectasia-mutated (Atm)/ATM and Rad3-related (Atr), for the progression of the G1/S cell cycle after DNA damage. Such changes indicated the combined effect of DDTs, PBDEs, and PCBs mixture that accumulated in cod tissue at Station 1, compared to the other two stations. An earlier study showed that exposure to organochlorines (OCs), particularly PCB congeners and 2,3,7,8-tetrachlorodibenzo-p-dioxin (TCDD) altered *brca1* gene expression (Rattenborg et al., 2002).

##### 4.1.4. Activation of NF- $\kappa$ B pathway to ROS production in cod ovary

Several environmental factors induce NADPH oxidase and mitochondrial respiratory chain to produce ROS that may either activate or inhibit Nf- $\kappa$ b pathways (Kabe et al., 2005). The expression levels of *nf- $\kappa$ b1* transcripts were higher at Kollevåg stations, and only the innermost station showed value above-set threshold fold-change (SI Fig. S4c). This expression pattern reflects the bioaccumulation profile of DDTs, PBDEs, and PCBs in cod tissues at Kollevåg stations. This observation was supported by previous findings showing that exposure to organochlorine pesticide (DDTs) induced cytotoxicity through the ROS-mediated Nf- $\kappa$ b pathways Jin et al. (Jin et al., 2014). Elsewhere, elevated glutathione peroxidase (GPx) and catalase (Cat) have been reported after exposure to persistent organic pollutants (Zhou et al., 2001). In contrast, an earlier investigation by Dale et al. (Dale et al., 2019) showed a significant decrease in glutathione s-transferase (Gst) and Cat activities in cod liver caged at Kollevåg innermost station. It was suggested that prolonged exposure to contaminants may deplete oxidative stress responses that were initially active (Benedetti et al., 2015). Contrary to enzymatic activity, our transcriptomics data showed DEGs that were annotated to ROS-induced cellular signaling pathways (SI Fig. S4c). For example, significant inhibition of kappa light polypeptide gene enhancer in B-cells, kinase beta (*ikkb*) was observed at Kollevåg stations. Elevated *ikkb* expression, further supports the activation of Nf- $\kappa$ b through canonical pathways (Ghosh and Karin, 2002). ROS also targeted the expression of mechanistic target of rapamycin kinase (*mtor*), which plays an important role in regulating folliculogenesis (Adhikari et al., 2009). The inhibition *mtor* involves other transcripts that also showed differential expression patterns at Kollevåg stations and is further discussed in SI Section 8.1.

MetaCore annotated differentially expressed fatty acid synthase (*fasn*) into a signaling pathway that responds to the presence of ROS in cells (SI Fig. S4c). In the present study, transcript count for *fasn* was significantly decreased at all Kollevåg stations. Decreased *fasn* levels indicated cellular protection by inhibiting the synthesis of fatty acid (Staal et al., 2006). Decreased expression of *fasn* is probably due to accumulated PAHs in cod tissues at all Kollevåg stations. Iwano et al. (Iwano et al., 2005) previously studied the effects of 3-MC on the expression of several transcripts in HepG2 cells, showing the down-regulation of *fasn* gene. Although there are available literature in support of PAHs effects on *fasn* expression, it should be noted that our data does not exclude the potential effects of other OCs that were also measured in cod, at significantly higher levels at Station 1, compared to the other stations. The high differential expression of *fasn* at Station 1, probably indicates the combined effect of both PAHs and OCs. The underlying mechanism for regulating *fasn* expression includes Forkhead Box O1 (Foxo1) protein (Liu et al., 2009), whose expression pattern correlated with *fasn* at Kollevåg stations.

##### 4.1.5. Crosstalk between mTOR signaling and androgen receptor (Ar)

POPs such as PCBs have been shown to alter the expression of transcripts involved in mTOR signaling (Frank et al., 2017). It is known that mTOR signaling regulates the phosphorylation status of Eif4e binding proteins (4e-bps) that are important for the initiation of the translation process. Low mTOR abundance hypophosphorylated 4e-bp1, allowing Eif4e to bind efficiently and block translation, and vice versa for high mTOR abundance (Hay and Sonenberg, 2004). Herein, cod

ovarian tissue at Kollevåg stations (1 and 3) showed a decrease in *mtor* levels that were predicted to modulate the process of translation (SI Fig. S4d). Such changes indicate the effects of OCs accumulated in cod tissues. However, station 3 does not show any significant changes in the levels of OCs, compared to the reference station. Among the list of analyzed compounds, only OH-PAH metabolites were present at all three stations that were assumed to be responsible for observed gene expression changes at station 3. This observation was strengthened further by the earlier findings of Zhang et al. (Zhang et al., 2019) showing that exposure to PAHs downregulated mTOR signaling pathways. Despite the high abundance of OH-PAH metabolites at all stations, station-specific differential expression of *mtor* represents possible concentration-specific effects. Likewise, the expression levels of eukaryotic initiation factor 4G (*eif4g*) follows the expression profile of *mtor* at Kollevåg stations. Both stations 1 and 3 showed significant decrease in expression values across set threshold fold-change (SI Fig. S4d). Functionally, Eif4g acts as a scaffold for Eif4a and Eif4e, positioning them on the ribosome near the 5' terminus of mRNA for translation (Pain, 1996).

MetaCore predicted "non-genomic action of the androgen receptor (Ar)" pathway associated with the biological process of translation and was significantly affected at all Kollevåg stations. Non-DNA binding action of Ar, through different second messengers, including Mapk were reported in different cell lines (Estrada et al., 2003). Herein, both *ar* and *mapk* transcripts showed significant transcript count at Kollevåg stations. This indicates that PAHs alone or in combination with OCs affects translational process in the cod ovary. A diverse array of compounds, from pesticide to PAHs can act as an androgen agonist, depending on their concentrations (Tamura et al., 2006).

#### 4.1.6. Epigenetic alterations of histone modulate transcript properties of cod ovarian genome

Some DEGs in the cod ovary at Kollevåg stations belong to pathways that are important for transcription. In female gonads, epigenetic regulation of gene expression is one, among other sensitive processes that respond to the presence of endocrine-disrupting chemicals in the environment (Uzumcu et al., 2012). Epigenetic alteration including post-translational modification of histone by lysine acetyltransferases (Kats) modulates transcription of genes (Kori et al., 2017). Acetylation disrupts the interaction between histone and DNA, as well as between neighboring nucleosomes to provide a conducive environment for transcription (Zhang et al., 2017). Deacetylase, on the other hand, function differently (Wang et al., 2009). Herein, both acetylase (*kat6a* and *kat6b*) and deacetylase, histone deacetylase 7b (*hdac7*) transcripts were reciprocally expressed, with the former showing decreased transcript count at contaminated Kollevåg sites. Mainly, the innermost station 1, ranked highest in differential expression pattern (SI Fig. S4e). Observed changes in the expression of transcripts are probably due to complex mixture of DDTs, PBDEs and PCBs that were present in cod tissues at Station 1, than other stations. Earlier, Casati, et al. (Casati et al., 2012) showed the induction of deacetylase machinery to PCBs mixture. Other components of the deacetylase complex were also differentially expressed at Kollevåg stations and discussed in detail in SI Section 8.2.

Other mechanisms that epigenetically regulate the expression of transcripts, including methylation at histone lysine residue; H3K9, H3K27, and H4K20 also suppress the expression of genes (Varier and Timmers, 2011). The ovarian profile showed significantly higher levels of histone methylase (*suv39h1* and *dnmt3b*) with a concomitant decrease in the expression of demethylase (*kdm5a*, *kdm5b*, and *kdm6a*) transcripts (SI Fig. S4e). The majority of these transcripts showed the highest differential expression at Station 1, followed by Station 3. Such changes suggest the possible effects of OCs, accumulated in cod tissues. However, station 3 does not show any significant changes in the levels of OCs, compared to the reference station. Among the list of analyzed compounds, only OH-PAH metabolites were present at all three stations and

were assumed to be responsible for the observed changes in the transcript expression patterns observed at station 3.

#### 4.1.7. Ovarian immunomodulatory responses

It has been reported that exposure of fish to anthropogenic chemicals effect immune responses in gonadal tissues (Colli-Dula et al., 2014). The present study also showed modulation of immune responses in the cod ovary to contaminants at Kollevåg stations. For example, Toll-like receptors (TLrs) represent an important immune responsive element, expressed in teleost gonadal tissue (Sanchez-Hernandez et al., 2013). Their response in gonads is sensitive to the presence of anthropogenic contaminants in the environment (Cabas et al., 2013). Herein, the highest transcriptome expression for *tlr8*, *tlr9*, and *tlr22* mRNA were observed at the Kollevåg Stations 1 > 2 (SI Table S1). Expression levels of *tlrs* at the two innermost stations (Station 1 and 2) follow the gradient of OCs, particularly PCBs. Earlier, Cuesta, et al. (Cuesta et al., 2008) reported higher transcript count of *tlr9* gene to organochlorine pesticides in gilthead seabream (*Sparus aurata* L.). Activated TLrs produce changes in the expression of transcripts responsible for the production of pro-inflammatory cytokines (Kumar et al., 2009). MetaCore predicted some pathways that are associate with cytokines signaling through Il-1, -3, -4, -6, -7, -8, -9 and -11 receptors (SI Fig. S6). The extended discussion of TLrs and the production of pro-inflammatory cytokines are presented in SI Section 8.3.

In this study, MetaCore also suggested alternative, classical and lectin induced complement pathways that are affected at Kollevåg stations. The alternative complement pathway was significantly affected at station 1 and 2, but the classical and lectin induced complement pathways were only affected at station 1. Station-specific responses reflect contaminant differences in the environments. Fish from the innermost station, accumulated significantly higher amounts of PCBs, DDTs, and PBDEs, suggesting their combined effects on complement pathways more than PAHs alone. It has been reported that DDTs modulate the complement system.51 Earlier, Colli-Dula et al. (Colli-Dula et al., 2014) reported that these pathways were affected in fish ovary after exposure to anthropogenic chemicals. Since complement C3 (C3) is the central molecule of the complement cascade, activation of C3 reflects the status of complement activation (Sahu and Lambris, 2001). Herein, *c3* and complement component 8, beta polypeptide (*c8b*) transcripts were differentially expressed and have been previously associated with humoral and inflammatory responses in fish (SI Table S1). Taking into account information of all immune-related pathways, the majority of whom followed the trend of high significant FDR value at Station 1. than the other two stations (SI Fig. S6). This indicates that the presence of organochlorine and organobromine mixture, most significantly target the immune system. Earlier, Martyniuk, et al. (Martyniuk et al., 2016) reported that largemouth bass (*Micropterus salmoides*) ovarian immune system were altered by exposure to organochlorine pesticides.

#### 4.1.8. Lipid metabolism (LM)

It has been reported that varying levels of ovarian lipids of maturing cod indicate gonadal lipid dynamics that are most preferably linked with reproductive performance (Rojbek et al., 2012). Relating transcriptome data with the lipid metabolite profile was evaluated by determining the levels of lipids in cod ovary from Kollevåg and reference stations. Cholesterol is a precursor for ovarian steroidogenesis. High amount of cholesterol induces endoplasmic reticulum (ER) associated fatty acyl CoA, cholesterol acyltransferase to convert cholesterol into esterified adduct for storage as lipid droplets (LDs) (Walther and Farese, 2009). Particularly for steroidogenic cells, CE-rich LDs are the primary source of cholesterol for steroidogenesis (Kraemer et al., 2013). Herein, CE molecules were significantly higher at station 3, but no changes were observed at station 1 and 2 (SI Section 5.3). This observation reciprocally correlates with plasma E2 levels in fish (Dale et al., 2019). As reported earlier, ovarian CE content depletes with estrogen stimulation, thus satisfying the demand for a substrate (Gibori et al., 1984).



Therefore, high CE levels were measured at Station 3. Furthermore, the associated protein vimentin (*vim*) and steroidogenic pathway enzyme genes such as *cyp17a1* and *cyp19a1* mRNA, showed significant increases that paralleled the contaminant gradient. Particularly, *cyp17a1* showed a clear trend, gradually decreasing from innermost to outermost stations. Among the levels of contaminants that bioaccumulated in cod tissues,  $\Sigma$ PCB-7 follows the expression profile of steroidogenic pathway enzyme transcripts and other transcripts that are important for cholesterol metabolism. Earlier investigations also observed a similar relationship between PCB congeners on E2 secretion and aromatase activity (Gregoraszcuk et al., 2003; Wojtowicz et al., 2005).

Sphingolipid is another important lipid class that plays an important role in vast number of physiological processes, particularly adrenal and gonadal steroidogenesis (Ozbay et al., 2006). As of cholesterol, sphingolipid metabolites were differentially present in the ovary of cod at Kollevåg stations. Contaminated Kollevåg Station 1 showed significant decreases in both sphingomyelin (SM) and diacylglycerol (DG), with increased levels of phosphatidylcholine (PC). Whereas, the other two stations showed, significantly higher levels of both DG and PC. Inter-station comparison between station 1 and 3 showed that the latter had higher levels of both SM and DG. However, SM levels were not significantly different from the reference station (SI Section 5.2). Earlier, Ding et al. (Ding et al., 2008) found a direct association between SM and DG concentrations. Sphingomyelin synthase (*Sms*) overexpression leads to high levels of both SM and DG. On the other hand, sphingomyelinases (*SMase*) catalyzes the transfer of phosphorylcholine (PPC) group from SM to DG, producing phosphatidylcholine (PC) (Lucki and Sewer, 2012). Such changes might be due to differential burden of contaminants at the Kollevåg stations. As PAH metabolites were significantly higher at all stations, we expected that changes in sphingolipid metabolism will produce SM as reported earlier by Potratz et al. (Potratz et al., 2016) The abundance of sphinganine at Station 1 indicate a shift from sphingolipid metabolism to ceramide (Cer) through de novo biosynthesis (Lucki and Sewer, 2012), where additional compounds including PCBs, DDTs, and PBDEs may have masked PAH effects. Exposure of rat to PCB153 showed significant changes in liver Cer (Pierucci et al., 2017).

Besides PC species, that are common among stations, other phospholipids including PE was significantly higher at Station 3. Previously, Lykidis (2007) summarized de novo phospholipid biosynthesis that initially starts with phosphatidic acid (PA), intermediately involving DG and leading to the production of PC, PE, PG, among others. Phospholipid moieties also undergo interconversion depending on the availability of enzymes (Hazel and Williams, 1990). These metabolic changes clearly show differences in cod response to contaminant levels at Kollevåg stations. In marine fish species, reproductive success is strongly affected by the quality of lipids, i.e. the fatty acid composition incorporated into oocyte (Wiegand, 1996). Polyunsaturated fatty acids (PUFA), a major dietary factor for successful reproduction, is proportionally higher in phospholipids than in triacylglycerols (TG) (Tocher and Sargent, 1984). Arachidonic acid (ARA) plays an important role in regulating reproduction in teleosts (Norberg et al., 2017). In our study, both station 1 and 2 showed significantly higher levels of ovarian phospholipase A2 group 4a (*pla2g4a*) transcripts which alter lipid metabolism by hydrolyzing membrane phospholipids to ARA in the ovary. ARA supplementation was shown to produce profound effects on reproductive performances of Japanese flounder (*Paralichthys olivaceus*) (Furuita et al., 2003), while cod showed inconsistent results towards ARA. Fecundity decreases with increasing supplementation of ARA (Norberg et al., 2017). In addition, there is crosstalk between free ARA and intracellular calcium mobilization. Low concentrations of free ARA mimics the role of inositol 1,4,5-triphosphate (IP3) and induces  $Ca^{2+}$  release from the endoplasmic reticulum. Further, high free ARA releases  $Ca^{2+}$  from the mitochondria and subsequently alters the transfer of cholesterol to mitochondria for steroidogenesis (Mercuré and Van Der Kraak, 1996).

Fish caged at polluted Kollevåg stations showed stimulation of free

ARA that was compensated by decreasing the expression of inositol 1,4,5-triphosphate receptor, type 1b and 2 (*itpr1b* and *itpr2*). Alongside, high expression of cyclooxygenase (*ptgs1*) stimulates ARA to induce testosterone production (Van Der Kraak and Chang, 1990). However, signalling through 5-hydroxytryptamine receptor 2A (Htr2A) has been suggested as an important receptor for the synthesis of ARA, as was shown in invertebrate gonads (Amireault and Dubé, 2005). In addition, ROS-mediated canonical pathways mobilize the release of  $Ca^{2+}$  from endoplasmic reticulum that involves ligand-independent transactivation of Pdgfr that further associates with phospholipase C, gamma 2 (Plc $\gamma$ 2) and protein kinase C delta (Prkc $\delta$ ) (Saito et al., 2002). ROS also induces Egr activation that augments Pdgfr response (Eguchi et al., 1998). All these protein transcripts showed significant difference in their transcript levels at Kollevåg stations, relative to the reference station.

Cod ovary from station 1 showed significant decrease in the expression of apolipoprotein transcripts such as - *apoa1*, *apoa2*, *apob*, and *apoc1* through increasing expression levels of *ppar- $\gamma$* . Such changes might be related to the effect of PCBs, DDTs, and PBDEs that were bioaccumulated in cod tissues at station 1, compared to other two stations. Apolipoproteins, particularly ApoB, has homology with Vtg and plays an important role in trafficking lipids into the oocyte (Li et al., 2003). The presence of OCPs and PCBs oxidizes the low-density lipoprotein (LDL) molecules (Kumar et al., 2014). Relevant to this, it is possible that homeostatic mechanisms prevent their access to ovarian tissue through decreased expression of apolipoprotein transcripts. In addition, *apo* transcript expression may also explain some of the changes in upstream transcription factors, including Hnf4- $\alpha$  and Nr0b2 (Ladías et al., 1992; Sudhakumari and Senthilkumaran, 2013). Despite the high transcript count of *nr0b2*, no effect on *apob* was observed at station 2, suggesting that other confounding factors may play a role in regulating their expression patterns. It has been reported that ox-LDL was able to activate Ppar- $\gamma$  and affecting steroid metabolism (Sikder et al., 2018).

#### 4.1.9. Other biological processes

Pathways associated with other biological processes including cell adhesion, epithelial-to-mesenchymal transition (EMT) and cytoskeleton remodelling were significantly affected and extensively discussed in the SI Section 8.4, 8.5 and 8.6 respectively. In brief, our data represented a set of differentially expressed transcripts that contribute structurally and functionally for the components of extracellular matrix (ECM) whose modulation leads to serious consequences for survival, proliferation, and steroidogenesis of granulosa cells as reported earlier by Le Bellego et al. (Le Bellego et al., 2005) Likewise, folliculogenesis regulatory EMT is also modulated because of high transcript count of mesenchymal protein vimentin (*Vim*) at Kollevåg stations. The EMT findings were strengthened further by the observed alteration in biological pathways responsible for cytoskeleton remodelling.

#### 4.2. Conclusions and significance

The application of quantitative transcriptomics, and lipidomics have been used in performing risk assessment and ecosystem quality monitoring of the Kollevåg capped dumping site, using cod ovarian endocrinology and developmental physiology as a model biological system. We have demonstrated, for the first time in any fish species or lower vertebrate, a novel and “real-time” evidence of reproductive effects of contaminant leakage from a capped solid waste marine dumpsite. Thus, our data substantiated previous finding showing that contaminant bioaccumulation at the study sites paralleled significant increases in the number of DEGs. Although, the number of DEGs is different, they shared common biological processes that may potentially affect reproductive performance. Overall, our findings showed a direct link between contaminant burden and gonado-toxicological responses in cod caged at the capped waste dumpsite.

## Author contributions

Essa A. Khan, Anders Goksøyr, Fekadu Yadetie, and Augustine Arukwe. designed the study; Essa A. Khan, Zdenka Bartosova, and Augustine Arukwe performed Laboratory analysis; Essa A. Khan, Xiaokang Zhang, Eileen M. Hanna, Zdenka Bartosova, Inge Jonassen, and Augustine Arukwe. analyzed data; and Essa A. Khan and Augustine Arukwe. prepared manuscript draft. All authors proofread the manuscript.

## Declaration of competing interest

The authors have no competing interests.

## Acknowledgments

We thank the Genomics Core Facility (GCF) at the Department of Clinical Science, University of Bergen, Norway to sequence Cod transcriptome. We thank the Mass Spectrometry Lab at the Faculty of Natural Science, NTNU, Norway to perform UPC<sup>2</sup>-MS/MS lipidomic analysis. We would like to acknowledge Susana Villa Gonzalez for help with data processing and lipid identification. Partial results from this study was presented at the 20th meeting of Pollutant Responses in Marine Organisms (PRIMO20) in Charleston, SC, USA, and Digital Life conference 2019, Tromsø Norway.

## Appendix A. Supplementary data

Supplementary data to this article can be found online at <https://doi.org/10.1016/j.envres.2020.109906>.

## Funding

This work was supported by the Research Council of Norway to the Centre for Digital Life Norway (DLN) project dCod 1.0 [grant number 248840]. The sequencing project at GCF is supported in part by major grants from the Research Council of Norway (grant no. 245979/F50) and Trond Mohn Stiftelse (grant no. BFS2016-genom).

## References

- Adhikari, D., Zheng, W., Shen, Y., Gorre, N., Hämäläinen, T., Cooney, A.J., Huhtaniemi, I., Lan, Z.-J., Liu, K., 2009. Tsc/mTORC1 signaling in oocytes governs the quiescence and activation of primordial follicles. *Hum. Mol. Genet.* 19 (3), 397–410.
- Amireault, P., Dubé, F., 2005. Serotonin and its antidepressant-sensitive transport in mouse cumulus-oocyte complexes and early embryos. *Biol. Reprod.* 73 (2), 358–365.
- Arukwe, A., Goksøyr, A., 2003. Eggshell and egg yolk proteins in fish: hepatic proteins for the next generation: oogenesis, population, and evolutionary implications of endocrine disruption. *Comp. Hepatol.* 2 (1), 4.
- Benedetti, M., Giuliani, M.E., Regoli, F., 2015. Oxidative metabolism of chemical pollutants in marine organisms: molecular and biochemical biomarkers in environmental toxicology. *Ann. N. Y. Acad. Sci.* 1340 (1), 8–19.
- Boone, D.L., Tsang, B.K., 1998. Caspase-3 in the rat ovary: localization and possible role in follicular atresia and luteal regression. *Biol. Reprod.* 58 (6), 1533–1539.
- Cabas, I., Chaves-Pozo, E., Garcia-Alcazar, A., Meseguer, J., Mulero, V., Garcia-Ayala, A., 2013. The effect of 17alpha-ethynylestradiol on steroidogenesis and gonadal cytokine gene expression is related to the reproductive stage in marine hermaphrodite fish. *Mar. Drugs* 11 (12), 4973–4992.
- Casati, L., Sendra, R., Colciago, A., Negri-Cesi, P., Berdasco, M., Esteller, M., Celotti, F., 2012. Polychlorinated biphenyls affect histone modification pattern in early development of rats: a role for androgen receptor-dependent modulation? *Epigenomics* 4 (1), 101–112.
- Chen, X., Xie, M., Liu, D., Shi, K., 2015. Downregulation of microRNA-146a inhibits ovarian granulosa cell apoptosis by simultaneously targeting interleukin-1 receptor-associated kinase and tumor necrosis factor receptor-associated factor 6. *Mol. Med. Rep.* 12 (4), 5155–5162.
- Chrysikou, L., Gemenetzis, P., Kouras, A., Manoli, E., Terzi, E., Samara, C., 2008. Distribution of persistent organic pollutants, polycyclic aromatic hydrocarbons and trace elements in soil and vegetation following a large scale landfill fire in northern Greece. *Environ. Int.* 34 (2), 210–225.
- Colli-Dula, R.-C., Martyniuk, C.J., Kroll, K.J., Prucha, M.S., Kozuch, M., Barber, D.S., Denslow, N.D., 2014. Dietary exposure of 17-alpha ethynylestradiol modulates physiological endpoints and gene signaling pathways in female largemouth bass (*Micropterus salmoides*). *Aquat. Toxicol.* 156, 148–160.
- Cuddihy, A.R., Li, S., Tam, N.W.N., Wong, A.H.-T., Taya, Y., Abraham, N., Bell, J.C., Koromilas, A.E., 1999. Double-stranded-RNA-activated protein kinase PKR enhances transcriptional activation by tumor suppressor p53. *Mol. Cell Biol.* 19 (4), 2475–2484.
- Cuesta, A., Meseguer, J., Esteban, M.A., 2008. Effects of the organochlorines p, p'-DDE and lindane on gilthead seabream leucocyte immune parameters and gene expression. *Fish Shellfish Immunol.* 25 (5), 682–688.
- Dale, K., Müller, M.B., Tairova, Z., Khan, E.A., Hatlen, K., Grung, M., Yadetie, F., Lille-Langøy, R., Blaser, N., Skaug, H.J., Lyche, J.L., Arukwe, A., Karlsen, O.A., Goksøyr, A., 2019. Contaminant accumulation and biological responses in Atlantic cod (*Gadus morhua*) caged at a capped waste disposal site in Kollevåg, Western Norway. *Mar. Environ. Res.* 145, 39–51.
- Davis, V.L., Couse, J.F., Goulding, E., Power, S., Eddy, E., Korach, K., 1994. Aberrant reproductive phenotypes evident in transgenic mice expressing the wild-type mouse estrogen receptor. *Endocrinology* 135 (1), 379–386.
- Ding, T., Li, Z., Hailemariam, T., Mukherjee, S., Maxfield, F.R., Wu, M.P., Jiang, X.C., 2008. SMS overexpression and knockdown: impact on cellular sphingomyelin and diacylglycerol metabolism, and cell apoptosis. *J. Lipid Res.* 49 (2), 376–385.
- Eguchi, S., Numaguchi, K., Iwasaki, H., Matsumoto, T., Yamakawa, T., Utsunomiya, H., Motley, E.D., Kawakatsu, H., Owada, K.M., Hirata, Y., 1998. Calcium-dependent epidermal growth factor receptor transactivation mediates the angiotensin II-induced mitogen-activated protein kinase activation in vascular smooth muscle cells. *J. Biol. Chem.* 273 (15), 8890–8896.
- Estrada, M., Espinosa, A., Müller, M., Jaimovich, E., 2003. Testosterone stimulates intracellular calcium release and mitogen-activated protein kinases via a G protein-coupled receptor in skeletal muscle cells. *Endocrinology* 144 (8), 3586–3597.
- Fabbro, M., Savage, K., Hobson, K., Deans, A.J., Powell, S.N., McArthur, G.A., Khanna, K. K., 2004. BRCA1-BARD1 complexes are required for p53Ser-15 phosphorylation and a G1/S arrest following ionizing radiation-induced DNA damage. *J. Biol. Chem.* 279 (30), 31251–31258.
- Folch, J., Lees, M., Sloane Stanley, G., 1957. A simple method for the isolation and purification of total lipides from animal tissues. *J. Biol. Chem.* 226 (1), 497–509.
- Frank, D.F., Miller, G.W., Connon, R.E., Geist, J., Lein, P.J., 2017. Transcriptomic profiling of mTOR and ryanodine receptor signaling molecules in developing zebrafish in the absence and presence of PCB 95. *PeerJ* 5, e4106.
- Furuita, H., Yamamoto, T., Shima, T., Suzuki, N., Takeuchi, T., 2003. Effect of arachidonic acid levels in broodstock diet on larval and egg quality of Japanese flounder *Paralichthys olivaceus*. *Aquaculture* 220 (1–4), 725–735.
- Ghosh, S., Karin, M., 2002. Missing pieces in the NF-κB puzzle. *Cell* 109 (2), S81–S96.
- Gibori, G., Chen, Y.D., Khan, I., Azhar, S., Reaven, G.M., 1984. Regulation of luteal cell lipoprotein receptors, sterol contents, and steroidogenesis by estradiol in the pregnant rat. *Endocrinology* 114 (2), 609–617.
- Goldberg, E.D., 1981. Oceans as waste space: the argument. *Oceanus* 24 (1), 2–9.
- Gregoraszcuk, E., Grochowalski, A., Chrzyszcz, R., Wegiel, M., 2003. Congener-specific accumulation of polychlorinated biphenyls in ovarian follicular wall follows repeated exposure to PCB 126 and PCB 153. Comparison of tissue levels of PCB and biological changes. *Chemosphere* 50 (4), 481–488.
- Hamilton, P.B., Rolshausen, G., Uren Webster, T.M., Tyler, C.R., 2017. Adaptive capabilities and fitness consequences associated with pollution exposure in fish. *Philos. Trans. R. Soc. Lond. B Biol. Sci.* 372 (1712), 20160042.
- Hay, N., Sonenberg, N., 2004. Upstream and downstream of mTOR. *Gene Dev.* 18 (16), 1926–1945.
- Hazel, J.R., Williams, E.E., 1990. The role of alterations in membrane lipid composition in enabling physiological adaptation of organisms to their physical environment. *Prog. Lipid Res.* 29 (3), 167–227.
- He, X., Jing, Y., Wang, J., Li, K., Yang, Q., Zhao, Y., Li, R., Ge, J., Qiu, X., Li, G., 2015. Significant accumulation of persistent organic pollutants and dysregulation in multiple DNA damage repair pathways in the electronic-waste-exposed populations. *Environ. Res.* 137, 458–466.
- Iwano, S., Nukaya, M., Saito, T., Asanuma, F., Kamataki, T., 2005. A possible mechanism for atherosclerosis induced by polycyclic aromatic hydrocarbons. *Biochem. Biophys. Res. Commun.* 335 (1), 220–226.
- Jin, X., Song, L., Liu, X., Chen, M., Li, Z., Cheng, L., Ren, H., 2014. Protective efficacy of vitamins C and E on p, p'-DDT-induced cytotoxicity via the ROS-mediated mitochondrial pathway and NF-κB/FasL pathway. *PLoS One* 9 (12).
- Kabe, Y., Ando, K., Hirao, S., Yoshida, M., Handa, H., 2005. Redox regulation of NF-κB activation: distinct redox regulation between the cytoplasm and the nucleus. *Antioxidants Redox Signal.* 7 (3–4), 395–403.
- Kori, Y., Sidoli, S., Yuan, Z.-F., Lund, P.J., Zhao, X., Garcia, B.A., 2017. Proteome-wide acetylation dynamics in human cells. *Sci. Rep.* 7 (1), 10296.
- Kraemer, F.B., Khor, V.K., Shen, W.J., Azhar, S., 2013. Cholesterol ester droplets and steroidogenesis. *Mol. Cell. Endocrinol.* 371 (1–2), 15–19.
- Kroupova, H., Trubiroha, A., Wuertz, S., Kloas, W., 2011. Stage-dependent differences in RNA composition and content affect the outcome of expression profiling in roach (*Rutilus rutilus*) ovary. *Comp. Biochem. Physiol., Part A Mol. Integr. Physiol.* 159 (2), 141–149.
- Kumar, H., Kawai, T., Akira, S., 2009. Toll-like receptors and innate immunity. *Biochem. Biophys. Res. Commun.* 388 (4), 621–625.
- Kumar, J., Lind, P.M., Salihovic, S., van Bavel, B., Lind, L., Ingelsson, E., 2014. Influence of persistent organic pollutants on oxidative stress in population-based samples. *Chemosphere* 114, 303–309.
- Ladias, J.A., Hadzopoulou-Cladaras, M., Kardassis, D., Cardot, P., Cheng, J., Zannis, V., Cladaras, C., 1992. Transcriptional regulation of human apolipoprotein genes ApoB,

- ApoCIII, and ApoAII by members of the steroid hormone receptor superfamily HNF-4, ARP-1, EAR-2, and EAR-3. *J. Biol. Chem.* 267 (22), 15849–15860.
- Le Bellego, F., Fabre, S., Pisselet, C., Monniaux, D., 2005. Cytoskeleton reorganization mediates alpha6beta1 integrin-associated actions of laminin on proliferation and survival, but not on steroidogenesis of ovine granulosa cells. *Reprod. Biol. Endocrinol.* 3 (1), 19.
- Li, A., Sadasivam, M., Ding, J.L., 2003. Receptor-ligand interaction between vitellogenin receptor (VtgR) and vitellogenin (Vtg), implications on low density lipoprotein receptor and apolipoprotein B/E. The first three ligand-binding repeats of VtgR interact with the amino-terminal region of Vtg. *J. Biol. Chem.* 278 (5), 2799–2806.
- Lim, J., Kong, W., Lu, M., Luderer, U., 2016. The mouse fetal ovary has greater sensitivity than the fetal testis to benzo [a] pyrene-induced germ cell death. *Toxicol. Sci.* 152 (2), 372–381.
- Lisa, M., Holčapek, M., 2015. High-throughput and comprehensive lipidomic analysis using ultrahigh-performance supercritical fluid chromatography–mass spectrometry. *Anal. Chem.* 87 (14), 7187–7195.
- Liu, Z., Rudd, M.D., Hernandez-Gonzalez, I., Gonzalez-Robayna, I., Fan, H.-Y., Zeleznik, A.J., Richards, J.S., 2009. FSH and FOXO1 regulate genes in the sterol/steroid and lipid biosynthetic pathways in granulosa cells. *Mol. Endocrinol.* 23 (5), 649–661.
- Lucki, N.C., Sewer, M.B., 2012. Nuclear sphingolipid metabolism. *Annu. Rev. Physiol.* 74, 131–151.
- Lykidis, A., 2007. Comparative genomics and evolution of eukaryotic phospholipid biosynthesis. *Prog. Lipid Res.* 46 (3–4), 171–199.
- Martyniuk, C.J., Prucha, M.S., Doperalski, N.J., Antczak, P., Kroll, K.J., Falciani, F., Barber, D.S., Denslow, N.D., 2013. Gene expression networks underlying ovarian development in wild largemouth bass (*Micropterus salmoides*). *PLoS One* 8 (3).
- Martyniuk, C.J., Doperalski, N.J., Feswick, A., Prucha, M.S., Kroll, K.J., Barber, D.S., Denslow, N.D., 2016. Transcriptional networks associated with the immune system are disrupted by organochlorine pesticides in largemouth bass (*Micropterus salmoides*) ovary. *Aquat. Toxicol.* 177, 405–416.
- Mercure, F., Van Der Kraak, G., 1996. Mechanisms of action of free arachidonic acid on ovarian steroid production in the goldfish. *Gen. Comp. Endocrinol.* 102 (1), 130–140.
- Norberg, B., Kleppe, L., Andersson, E., Thorsen, A., Rosenlund, G., Hamre, K., 2017. Effects of dietary arachidonic acid on the reproductive physiology of female Atlantic cod (*Gadus morhua* L.). *Gen. Comp. Endocrinol.* 250, 21–35.
- Orn, S., Yamani, S., Norrgren, L., 2006. Comparison of vitellogenin induction, sex ratio, and gonad morphology between zebrafish and Japanese medaka after exposure to 17alpha-ethinylestradiol and 17beta-trenbolone. *Arch. Environ. Contam. Toxicol.* 51 (2), 237–243.
- Ozbay, T., Rowan, A., Leon, A., Patel, P., Sewer, M.B., 2006. Cyclic adenosine 5'-monophosphate-dependent sphingosine-1-phosphate biosynthesis induces human CYP17 gene transcription by activating cleavage of sterol regulatory element binding protein 1. *Endocrinology* 147 (3), 1427–1437.
- Pain, V.M., 1996. Initiation of protein synthesis in eukaryotic cells. *Eur. J. Biochem.* 236 (3), 747–771.
- Pierucci, F., Frati, A., Squecco, R., Lenci, E., Vicenti, C., Slavik, J., Francini, F., Machala, M., Meacci, E., 2017. Non-dioxin-like organic toxicant PCB153 modulates sphingolipid metabolism in liver progenitor cells: its role in Cx43-formed gap junction impairment. *Arch. Toxicol.* 91 (2), 749–760.
- Potratz, S., Jungnickel, H., Grabiger, S., Tarnow, P., Otto, W., Fritsche, E., von Bergen, M., Luch, A., 2016. Differential cellular metabolite alterations in HaCaT cells caused by exposure to the aryl hydrocarbon receptor-binding polycyclic aromatic hydrocarbons chrysene, benzo [a] pyrene and dibenzo [a, i] pyrene. *Toxicol. Rep.* 3, 763–773.
- Rattenborg, T., Gjermansen, I., Bonefeld-Jørgensen, E.C., 2002. Inhibition of E2-induced expression of BRCA1 by persistent organochlorines. *Breast Cancer Res.* 4 (6), R12.
- Rhon-Calderón, E.A., Toro, C.A., Lomniczi, A., Galarza, R.A., Faletti, A.G., 2018. Changes in the expression of genes involved in the ovarian function of rats caused by daily exposure to 3-methylcholanthrene and their prevention by  $\alpha$ -naphthoflavone. *Arch. Toxicol.* 92 (2), 907–919.
- Røjbek, M.C., Jacobsen, C., Tomkiewicz, J., Støttrup, J.G., 2012. Linking lipid dynamics with the reproductive cycle in Baltic cod *Gadus morhua*. *Mar. Ecol. Prog. Ser.* 471, 215–234.
- Sahu, A., Lambris, J.D., 2001. Structure and biology of complement protein C3, a connecting link between innate and acquired immunity. *Immunol. Rev.* 180 (1), 35–48.
- Saito, S., Frank, G.D., Mifune, M., Ohba, M., Utsunomiya, H., Motley, E.D., Inagami, T., Eguchi, S., 2002. Ligand-independent trans-activation of the platelet-derived growth factor receptor by reactive oxygen species requires protein kinase C- $\delta$  and c-Src. *J. Biol. Chem.* 277 (47), 44695–44700.
- Sanchez-Hernandez, M., Chaves-Pozo, E., Cabas, I., Mulero, V., Garcia-Ayala, A., Garcia-Alcazar, A., 2013. Testosterone implants modify the steroid hormone balance and the gonadal physiology of gilthead seabream (*Sparus aurata* L.) males. *J. Steroid Biochem. Mol. Biol.* 138, 183–194.
- Sikder, K., Shukla, S.K., Patel, N., Singh, H., Rafiq, K., 2018. High fat diet upregulates fatty acid oxidation and ketogenesis via intervention of PPAR-gamma. *Cell. Physiol. Biochem. : international journal of experimental cellular physiology, biochemistry, and pharmacology* 48 (3), 1317–1331.
- Staal, Y.C., Van Herwijnen, M.H., van Schooten, F.J., van Delft, J.H., 2006. Modulation of gene expression and DNA adduct formation in HepG2 cells by polycyclic aromatic hydrocarbons with different carcinogenic potencies. *Carcinogenesis* 27 (3), 646–655.
- Sudhakumari, C., Senthilkumaran, B., 2013. Expression Profiling of Various Marker Genes Involved in Gonadal Differentiation of Teleosts: Molecular Understanding of Sexual Plasticity. Nova Biomedical, New York, NY, USA.
- Tamura, H., Ishimoto, Y., Fujikawa, T., Aoyama, H., Yoshikawa, H., Akamatsu, M., 2006. Structural basis for androgen receptor agonists and antagonists: interaction of SPEED 98-listed chemicals and related compounds with the androgen receptor based on an in vitro reporter gene assay and 3D-QSAR. *Bioorg. Med. Chem.* 14 (21), 7160–7174.
- Thorpe, J.E., 1994. Reproductive strategies in Atlantic salmon, *Salmo salar* L. *Aquaculture Fisher. Manage* 25, 77–87.
- Tocher, D.R., Sargent, J.R., 1984. Analyses of lipids and fatty acids in ripe roes of some northwest European marine fish. *Lipids* 19 (7), 492–499.
- Uzumcu, M., Zama, A.M., Oruc, E., 2012. Epigenetic mechanisms in the actions of endocrine-disrupting chemicals: gonadal effects and role in female reproduction. *Reprod. Domest. Anim.* 47, 338–347.
- Van Der Kraak, G., Chang, J.P., 1990. Arachidonic acid stimulates steroidogenesis in goldfish preovulatory ovarian follicles. *Gen. Comp. Endocrinol.* 77 (2), 221–228.
- Vanorny, D.A., Prasasya, R.D., Chalpe, A.J., Kilen, S.M., Mayo, K.E., 2014. Notch signaling regulates ovarian follicle formation and coordinates follicular growth. *Mol. Endocrinol.* 28 (4), 499–511.
- Variar, R.A., Timmers, H.M., 2011. Histone lysine methylation and demethylation pathways in cancer. *Biochim. Biophys. Acta* 1815 (1), 75–89.
- Vassenden, G., Johannessen, P., 2009. SAM E-Rapport.
- Walther, T.C., Farese Jr., R.V., 2009. The life of lipid droplets. *Biochim. Biophys. Acta* 1791 (6), 459–466.
- Wang, Z., Zang, C., Cui, K., Schones, D.E., Barski, A., Peng, W., Zhao, K., 2009. Genome-wide mapping of HATs and HDACs reveals distinct functions in active and inactive genes. *Cell* 138 (5), 1019–1031.
- Wiegand, M.D., 1996. Composition, accumulation and utilization of yolk lipids in teleost fish. *Rev. Fish Biol. Fish.* 6 (3), 259–286.
- Wojtowicz, A., Goch, M., Gregoraszczyk, E., 2005. Polychlorinated biphenyls (PCB 153 and PCB 126) action on conversion of 20-hydroxylated cholesterol to progesterone, androstenedione to testosterone, and testosterone to estradiol 17 $\beta$ . *Exp. Clin. Endocrinol. Diabetes* 113 (8), 464–470.
- Yeh, P.-Y., Chuang, S.-E., Yeh, K.-H., Song, Y.C., Cheng, A.-L., 2001. Nuclear extracellular signal-regulated kinase 2 phosphorylates p53 at Thr55 in response to doxorubicin. *Biochem. Biophys. Res. Commun.* 284 (4), 880–886.
- Zhang, X., Jonassen, I., 2020. RASflow: an RNA-Seq analysis workflow with Snakemake. *BMC Bioinf.* 21 (1), 1–9.
- Zhang, R., Erler, J., Langowski, J., 2017. Histone acetylation regulates chromatin accessibility: role of H4K16 in inter-nucleosome interaction. *Biophys. J.* 112 (3), 450–459.
- Zhang, Y., Yang, D., Yang, B., Li, B., Guo, J., Xiao, C., 2019. PM2.5 induces cell cycle arrest through regulating mTOR/P70S6K1 signaling pathway. *Exp. Ther. Med* 17 (6), 4371–4378.
- Zhou, L.Z.-H., Johnson, A.P., Rando, T.A., 2001. NF $\kappa$ B and AP-1 mediate transcriptional responses to oxidative stress in skeletal muscle cells. *Free Radic. Biol. Med.* 31 (11), 1405–1416.